PAPER

Inhibitory properties of saponin from *Eleocharis dulcis* peel against α-glucosidase†

Yipeng Gu, [a] Xiaomei Yang,[b] Chaojie Shang,[a] Truong Thi Phuong Thao[a] and Tomoyuki Koyama*[a]

The inhibitory properties towards α-glucosidase *in vitro* and elevation of postprandial glycemia in mice by the saponin constituent from *Eleocharis dulcis* peel were evaluated for the first time. Three saponins were isolated by silica gel and HPLC, identified as stigmasterol glucoside, campesterol glucoside and daucosterol by NMR spectroscopy. Daucosterol presented the highest content and showed the strongest α-glucosidase inhibitory activity with competitive inhibition. Static fluorescence quenching of α-glucosidase was caused by the formation of the daucosterol–α-glucosidase complex, which was mainly derived from hydrogen bonds and van der Waals forces. Daucosterol formed 7 hydrogen bonds with 4 residues of the active site and produced hydrophobic interactions with 3 residues located at the exterior part of the binding pocket. The maltose-loading test results showed that daucosterol inhibited elevation of postprandial glycemia in ddY mice. This suggests that daucosterol from *Eleocharis dulcis* peel can potentially be used as a food supplement for anti-hyperglycemia.

1. Introduction

α-Glucosidase hydrolyzes terminal non-reducing α-1,4-glycosidic bonds to release a glucose molecule, which is involved in glycometabolism and plays an important role in maintaining the normal physiological function of the body.[1–3] This enzyme is located in the brush border of the small intestine and catalyzes the hydrolysis of polysaccharides or oligosaccharides into glucose to induce postprandial hyperglycemia; by regulating this process, diabetic patients can control glucose uptake and suppress rapid rises of blood glucose levels to prevent the development of diabetes-associated complications.[4,5] Currently, the widely used clinical antidiabetic drugs are α-glucosidase inhibitors, such as acarbose, voglibose and miglitol, to inhibit the intestinal absorption of glucose, but the long-term administration of these agents may produce adverse side effects and high cost.[6,7] In search of appropriate hypoglycemic medications, attention has been focused on edible plants for several years, whose extracts contain bioactive components that demonstrate significant α-glucosidase inhibitory activity, such as L-arabinose, salacinol, mangiferin and soybean isoflavone.[8–12]

Eleocharis dulcis (also known as Chinese water chestnut), a perennial sedge belonging to the family Cyperaceae, is a common hydrophytic vegetable that grows in Japan, China, India and other Asian countries.[13,14] The edible corms are consumed as a fruit or vegetable, and also used to produce starch and canned foods.[15] In China, fresh-cut *Eleocharis dulcis* is very popular due to its unique sweet taste and medicinal properties. As a traditional Chinese medicine, the corm of *Eleocharis dulcis* has been applied to treat constipation, pharyngitis, laryngitis, hypertension and chronic nephritis.[16,17] However, a large amount of peel is produced as a waste product in fruit processing and accumulates, causing rot and serious environmental pollution.[18] It has been reported that twenty flavonoids isolated from *Eleocharis dulcis* peel show strong 2,2-diphenyl-1-picrylhydrazyl (DPPH) radical scavenging activity.[15] The ethanol extract from *Eleocharis dulcis* with high values of phenolic and flavonoids compounds showed an inhibitory value of 65.74% against α-glucosidase at a concentration of 2000 ppm.[19] However, there are currently few reports about saponins from *Eleocharis dulcis* peel. Saponins are widely distributed in natural medicines with various pharmacological activities, such as antimicrobial, antioxidant, antithrombotic, antitumor, hypoglycemic, *etc.*[20] Hence, this study aimed to research the saponin constituent in *Eleocharis dulcis* peel and evaluate its inhibition of α-glucosidase and elevation of postprandial glycemia in mice after maltose-loading for the first time, and it is expected to be applied in functional foods in the future.

[a]Laboratory of Nutraceuticals and Functional Foods Science, Graduate School of Marine Science and Technology, Tokyo University of Marine Science and Technology, 4-5-7 Konan, Minato, Tokyo 108-8477, Japan. E-mail: tskoyama@kaiyodai.ac.jp

[b]Institute of Food Science and Technology, Hezhou University, Hezhou 542899, China

2. Materials and methods

2.1 Materials

The fresh *Eleocharis dulcis* were purchased from the central agricultural product market of Hezhou (Hezhou, Guangxi

Province, China) and cleaned with water, and then the peels without decay and deterioration were collected and dried with a DHG series heating and drying oven (DHG-9140A, Keelrein, China) at 60 °C for 36 h. After this, the dried peels were ground by a universal high-speed grinder (DFY-600, Linda Machinery Co., Ltd, China) and stored for further extraction.

α-Glucosidase (EC 3.2.1.20) from yeast was purchased from Oriental Yeast Co., Ltd (Tokyo, Japan), and dissolved in 0.1 M sodium phosphate buffer of pH 7.4. Methanol, acetonitrile and distilled water as HPLC grade chemicals were purchased from Kanto Chemical Co., Inc. (Tokyo, Japan). Acarbose and *p*-nitrophenyl-α-D-glucopyranoside (*p*NPG) were purchased from Tokyo Chemical Industry Co., Ltd (Tokyo, Japan). A Glucose C-II Test Wako Kit was obtained from Fujifilm Wako Pure Chemical Industries, Ltd (Osaka, Japan). Pyridine-d_5 for NMR spectroscopy and maltose were purchased from Kanto Chemical Co., Inc. (Tokyo, Japan). All other reagents were of analytical purity.

2.2 Extraction and isolation of the saponin fraction

The dried materials of *Eleocharis dulcis* peel (1 kg) were combined with 5 L methanol and kept in an ultrasonic reactor (KQ5200DV, Kunshan, China) at 40 kHz and 60 °C for 2 h. The filtered methanol extracts were concentrated by a rotary evaporator (N1300DW, EYELA, Japan) and dried by a freeze-dryer (FDU2110, EYELA, Japan), and then suspended with 0.2 L of distilled water and partitioned with *n*-butanol (1 L) twice. The organic layer was collected and freeze-dried, and then these extracts were dissolved in methanol and five volumes of acetone were gradually added until complete precipitation. The precipitates were subjected to a silica gel column (4 cm × 11 cm), and eluted with *n*-hexane, ethyl acetate, methanol–ethyl acetate (v : v = 1 : 1) and methanol, at five times the column volume for each eluent. The separation process is illustrated in Fig. 1. A Bruker Advance 600 MHz spectrometer (Bruker, Germany) was used to obtain ¹H NMR spectra with pyridine-d_5 as the solvent. Fr.3 and Fr.4 were detected, which showed similar saponin signals
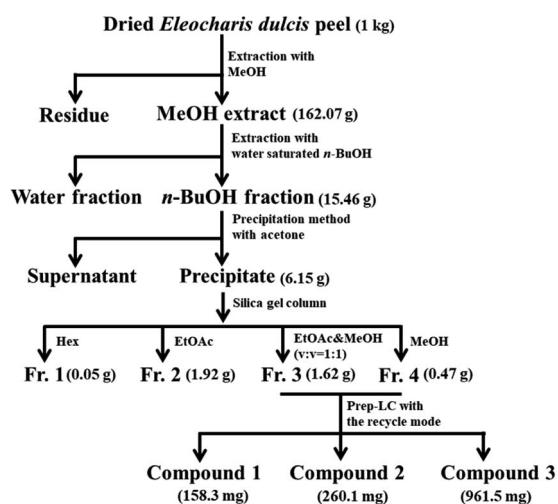

Fig. 1 Flowchart for the isolation of saponins from *Eleocharis dulcis* peel.

(Fig. S1A†). Furthermore, a Shimadzu HPLC System (Kyoto, Japan) equipped with a Develosil ODS HG-5 column (4.6 mm × 250 mm, Nomura Chemical, Japan) with isocratic elution of 100% methanol at 30 °C (wavelength: 210 nm, flow rate: 1 mL min⁻¹) also demonstrated no difference between the two saponin fractions (Fig. S1B†). Fr.3 and Fr.4 were combined and dried to obtain a powder (2.09 g).

2.3 Purification and structural elucidation of saponins

The powder of the saponin fraction was dissolved in methanol, and a Prep LC System (PU2080 Plus, JASCO, Japan) in recycling mode was used to purify the saponins. The ultraviolet absorption spectrum was obtained using a Develosil ODS HG-5 column (20 mm × 250 mm, Nomura Chemical, Japan) and eluted with 100% methanol at room temperature (wavelength: 210 nm, flow rate: 8 mL min⁻¹), and three components were collected in accordance with the chromatogram (Fig. S2†). After freeze-drying, compound **3** gave the highest amount with a total yield of 961.5 mg, achieving 0.10% overall recovery; the compound **1** yield was 158.3 mg (0.02%), and that of compound **2** was 260.1 mg (0.03%). The structures of all components were characterized by NMR spectroscopy techniques on a Bruker Advance 600 MHz spectrometer (Bruker, Germany). Accordingly, the three compounds were identified as stigmasterol glucoside (**1**), campesterol glucoside (**2**) and daucosterol (**3**), as shown in Fig. 2. Furthermore, the NMR data for the compounds were consistent with those reported in the literature.[21–25]

2.4 α-Glucosidase inhibitory activity assay *in vitro*

The α-glucosidase inhibitory activities were measured according to a slightly modified method reported by Zhang *et al.*[26] Several assay solutions containing 20 μL of α-glucosidase of 0.5 U mL⁻¹, 120 μL of phosphate buffer (pH 7.4) of 0.1 M, and 10 μL of dimethyl sulfoxide solution of saponin were prepared at various concentrations from 0 to 1 mg mL⁻¹ mixed in a 96-well microtiter plate. The plate was incubated at 37 °C for 10 min. The enzymatic reaction was initiated by adding 20 μL of 5 mM substrate *p*NPG solution in 0.1 M phosphate buffer of pH 7.4, and the final reaction mixture was incubated for 10 min at 37 °C. Subsequently, the absorbance of the reaction system was immediately transferred into a ThermoMax microplate reader (31139, Thermo, USA) and measured at 405 nm. The enzymatic activity assay without the saponin sample, which was replaced by dimethyl sulfoxide, was defined as the control, and that without α-glucosidase was used as a control blank to correct for background absorbance. The enzymatic inhibitory reaction system without enzyme was used as a sample blank. Acarbose were used as a positive control at different concentrations from 1 to 4 mg mL⁻¹. The median effective concentration for inhibition (IC₅₀) was measured, and the IC₅₀ value was the amount that gave a 50% decrease in α-glucosidase activity. The inhibitory activity was calculated using eqn (1). The best inhibitor was screened out and used in subsequent experiments.

$$\text{Inhibition } (\%) = 1 - \frac{A_{\text{sample}} - A_{\text{sample blank}}}{A_{\text{control}} - A_{\text{control blank}}} \times 100 \qquad (1)$$
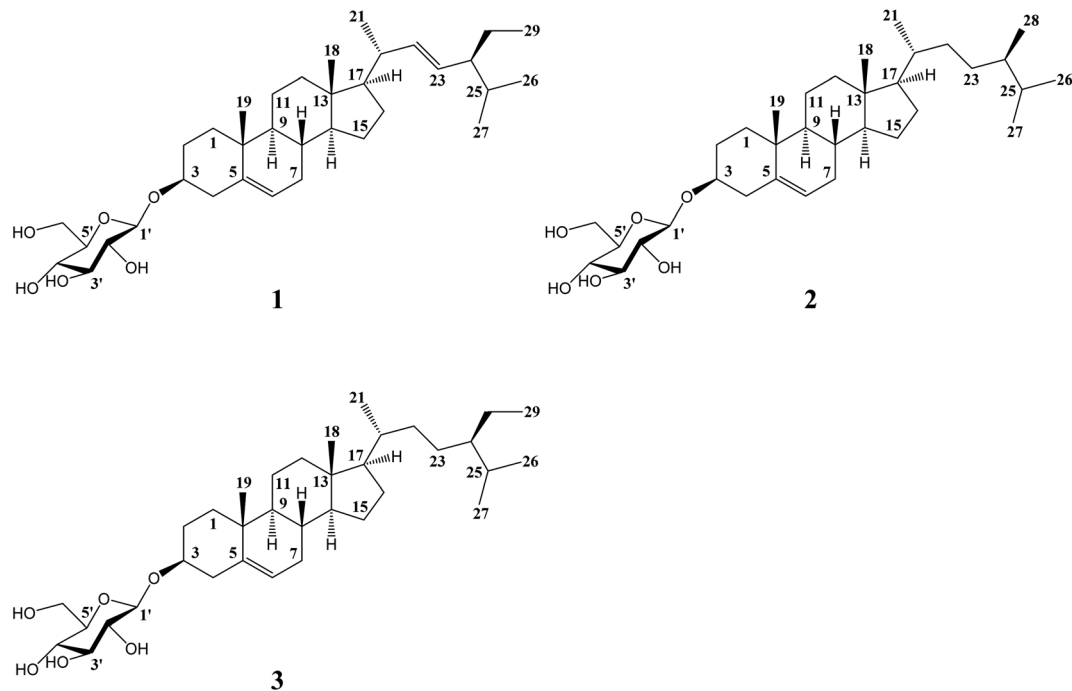
Fig. 2 The chemical structures of the three compounds isolated from *Eleocharis dulcis* peel. The structures from **1** to **3** are stigmasterol glucoside, campesterol glucoside and daucosterol, respectively.

2.5 Analysis of the inhibitory kinetics of α-glucosidase activity

The mechanism of α-glucosidase inhibition of the saponin sample was detected by analysis of the Michaelis–Menten kinetics equation,[27] as shown below:

$$V = V_{\max} \frac{[S]}{K_m + [S]} \qquad (2)$$

and in general, it was measured by the double reciprocal Michaelis–Menten equation, that is the Lineweaver–Burk plot, as follows:

$$\frac{1}{V} = \frac{K_m + [S]}{V_{\max}[S]} = \frac{K_m}{V_{\max}} \frac{1}{[S]} + \frac{1}{V_{\max}} \qquad (3)$$

In this equation, V is the initial rate of enzymatic reaction, $V_{\max}$ is the maximum value of reaction rate, and K_m and $[S]$ are the Michaelis–Menten constant and the concentration of substrate, respectively.

The concentration of the saponin sample as an α-glucosidase inhibitor was varied from 0 to 10 mg L^{-1}, and *p*NPG was the substrate of the enzymatic reaction at different concentrations (0, 0.2, 0.4, 0.8, 1.6 and 3.2 mM).

2.6 Fluorescence spectrum

A fluorescence spectrometer (F-4600, HITACHI, Japan) was used to analyze the fluorescence quenching of α-glucosidase by saponin. A series of 5 mL colorimetric tubes were injected with 100 μL of different concentrations of saponin sample and 2 mL

α-glucosidase (0.5 U mL^{-1}); then, these mixtures were diluted to the required volume with phosphate buffer (pH 7.4) of 0.1 M. The final concentrations of saponin varied from 0 to 20 mg L^{-1}. The tubes for reaction were kept at the temperature of 298, 303 and 310 K for 20 min. The fluorescence measurements were performed at the excitation wavelength of 280 nm, in the emission wavelength range of 300–400 nm, and excitation and emission slit widths of the fluorescence spectrophotometer were both 10 nm. Their synchronous fluorescence spectra were scanned with the excitation and emission slit widths at 5 nm in the wavelength range of 240–340 nm, with the excitation and emission wavelength interval (Δ*λ*) at 15 and 60 nm. The reaction system without α-glucosidase was subtracted to correct background fluorescence.

2.7 Molecular docking studies

The yeast α-glucosidase originated from *Saccharomyces cerevisiae* in this study, and the amino acid sequences were searched in the NCBI database and the α-glucosidase (*Saccharomyces cerevisiae*) sequence file (GenBank: KZV11524.1) was downloaded. However, its 3D structure has never been reported. In order to find an appropriate crystal structure for homology modeling, the BLAST algorithm was used to search for the protein sequence data in the Protein Data Bank (PDB, http://www.rcsb.org) and a known protein (ID: 3AXI_A) showed significant similarity, which exhibits 93% homology with this sequence. The 3D structure of the inhibitor was searched and obtained in the PubChem database (https://pubchem.ncbi.nlm.nih.gov). Its energy was minimized by UCSF Chimera-1.13.1 (RBVI, USA) with the AMBER force field. In the virtual screening with docking simulation, the

Table 1 α-Glucosidase inhibitory activities of the three compounds from *Eleocharis dulcis* peel[a]

	Isolated compounds			
Inhibitor	Stigmasterol glucoside (**1**)	Campesterol glucoside (**2**)	Daucosterol (**3**)	Acarbose
IC_{50} (mg L^{-1})	7.68 ± 0.17[#b]	10.03 ± 0.78[#a]	5.67 ± 0.14[#c]	91.50 ± 4.69

[a] Values are means $\pm$ SD, $n = 3$. [#]$p < 0.05$, compared with acarbose. [abc]$p < 0.05$, different letters indicate significance in isolated compounds.

homologous model was used as the protein receptor and the inhibitor as the ligand model. All of the solvent molecules and nonessential substructures were removed by PyMOL software (version: 2.2.0, DeLano Scientific LLC, USA), and non H-bonding hydrogen atoms and Gasteiger charges were added by AutoDock tools (version: 1.5.6, Scripps Research, USA). A semi-flexible docking method was used for the molecular docking of the receptor and ligand using AutoDock tools programs. The protein receptor was set to be rigid and the ligand was given rotatable bonds to remain flexible, a grid box of $66 \times 68 \times 70$ Å was defined and the grid spacing was 0.375 Å, and Lamarckian Genetic Algorithm (LGA, runs 20) was used for molecular docking to determine the ligand binding sites on the receptor. The energies of molecular docking, the positions of the hydrogen bonds and the hydrophobic interactions between α-glucosidase and the inhibitor were analyzed. The interaction between the inhibitor and α-glucosidase from the AutoDock output files was rendered with PyMOL.

2.8 Effect of inhibitor on blood glucose level in maltose-loaded mice

Thirty male mice (ddY, SLC, Japan), body weight 38 ± 2 g, were fasted for 20–24 hours after conventional raising for one week in an individual animal breeding system (LP-80 CCFL-6ARSS, NK System, Japan) under the conditions of 24 ± 1 °C and $50 \pm 10\%$ humidity with a 12 h light/dark cycle. All mice were divided randomly into 5 groups ($n = 6$) and used for the maltose-loading test, and the route of administration was gastric perfusion. Saponin and acarbose were dispersed or dissolved well in 1% sodium carboxymethylcellulose (CMC), and maltose was dissolved in distilled water. In the low, middle and high dose treatment groups, the mice were given 25, 50 and 100 mg kg^{-1} body weight of saponin 30 minutes in advance. Mice in the control group and positive control group were treated with an appropriate volume of 1% CMC and acarbose (100 mg kg^{-1} body weight), respectively. The mice in each group were given 1 g kg^{-1} body weight maltose. Specimens of blood were collected from the tail vein prior to oral maltose (0 min) and at 30, 60, 90, and 120 min after oral gavage, centrifuged at 8000 rpm for 3 min (Centrifuge MCD-2000, AS ONE, Japan), and the serum samples were collected. The serum glucose level was measured using a Glucose C-II Test Wako Kit based on absorbance at 490 nm wavelength.

2.9 Statistical analysis

Data are presented as the means $\pm$ standard deviation (SD) for *in vitro* experiments and as the means $\pm$ standard error of the mean (SEM) for *in vivo* experiments. Statistical analysis were performed by JMP 7.0.2 (SAS Institute Inc., Cary, NC, USA). The significance analysis of differences in inhibitory activity among α-glucosidase inhibitors was conducted by an unpaired Student's *t*-test ($p < 0.05$), and the blood glucose level of each group was ascertained by a Tukey–Kramer HSD test ($p < 0.05$).

3. Results and discussion

3.1 α-Glucosidase inhibitory activity

The inhibitory activities of α-glucosidase by the three compounds are summarized in Table 1. The three saponins provided potent inhibition of α-glucosidase with the IC_{50} values being 7.68 mg L^{-1} (stigmasterol glucoside), 10.03 mg L^{-1} (campesterol glucoside) and 5.67 mg L^{-1} (daucosterol), which were significantly stronger than that of acarbose (91.50 mg L^{-1}). In addition, daucosterol had the lowest IC_{50} value, indicating that it had the strongest inhibitory activity against α-glucosidase. The structures of the three saponins were quite similar (Fig. 2), and only slight differences indicated by the alkyl chains are shown; the number of unsaturated bonds and methylene groups affects the hydrophobicity of the molecule, which plays an important role in the interaction between small molecule drugs and proteins.[28–31] The higher molecular weight and unsaturation of daucosterol compared to the other two saponins could be related to its strongest inhibition. Moreover,
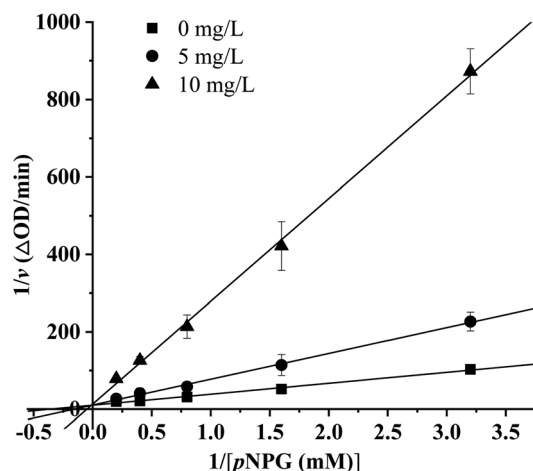

Fig. 3 The inhibition kinetics of α-glucosidase by daucosterol (pH 7.4, $T = 310$ K). Values are means $\pm$ SD, $n = 3$.
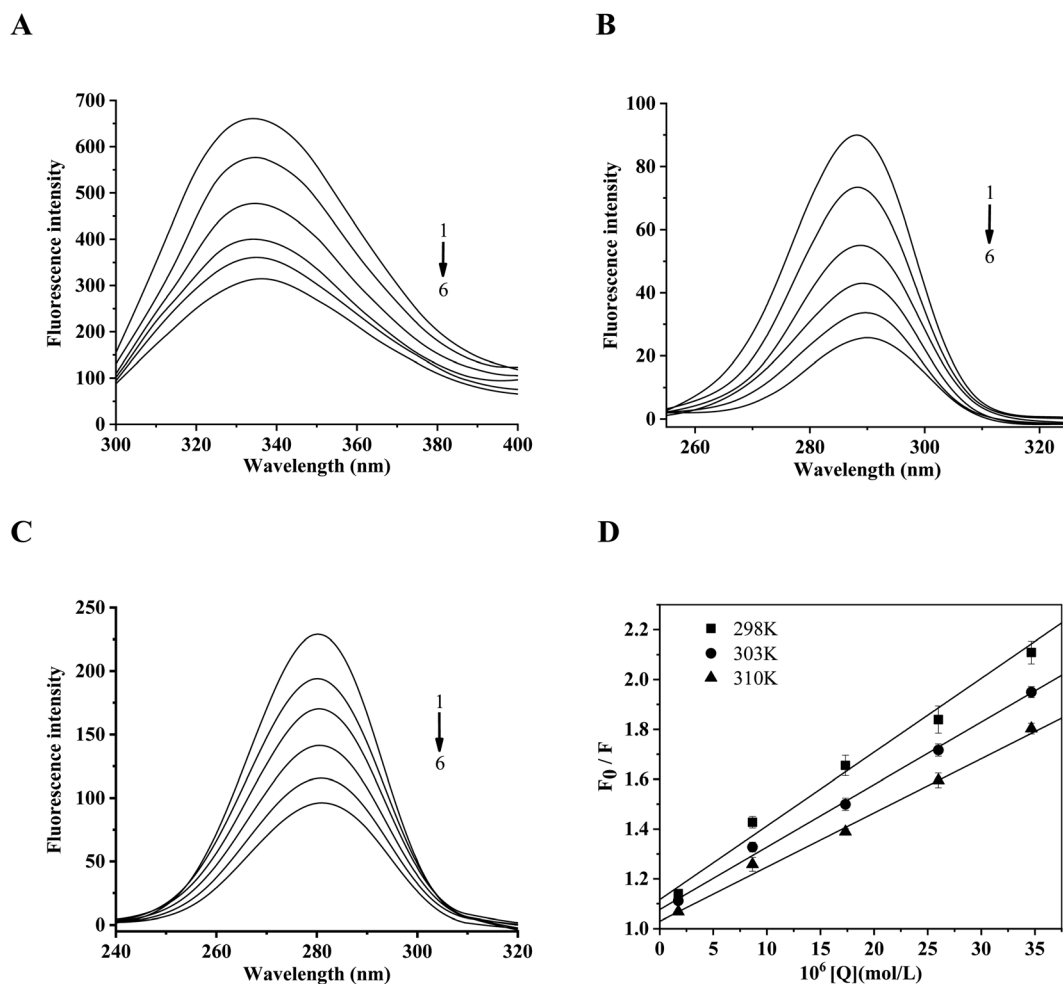
Fig. 4 The fluorescence quenching of α-glucosidase by daucosterol. (A–C) The fluorescence emission spectra (A) and the synchronous fluorescence spectra (B and C) of α-glucosidase in the presence of daucosterol at different concentrations (pH 7.4, T = 298 K). (A) λ_{ex} = 280 nm; (B) $\Delta\lambda$ = 15 nm; (C) $\Delta\lambda$ = 60 nm. The concentrations of daucosterol from 1 to 6 are 0.00, 1.00, 5.00, 10.00, 15.00 and 20.00 mg L^{-1}, respectively. (D) The linear-fitting graph of Stern–Volmer for the fluorescence quenching of α-glucosidase by daucosterol at different temperatures (pH 7.4, T = 298 K, 303 K, 310 K). λ_{ex} = 280 nm, λ_{em} = 334 nm. Values are means ± SD, n = 3. The concentrations of daucosterol are 0.00, 0.17, 0.87, 1.73, 2.60 and 3.47 × 10^{-5} mol L^{-1}, respectively.

daucosterol was the most abundant saponin isolated from *Eleocharis dulcis* peel, indicating that it was the major α-glucosidase inhibitory factor in the saponin fraction.

3.2 The inhibition kinetics of α-glucosidase

Lineweaver–Burk plots analysis was used to investigate the inhibition type according to the change of Michaelis–Menten constant (K_m) and the maximum value of reaction rate (V_{max}). In Fig. 3, the three fitting lines with different slopes intersected on the y axis, the reaction rate increased with the increasing concentration of the substrate, the value of $1/v$ rose in a dose-dependent manner, caused by the increase of $1/[p$NPG] being greater in the presence of daucosterol than in its absence. In the Lineweaver–Burk plot, the y intercept of the graph was equivalent to the inverse of V_{max}, and the x intercept of the graph was $-1/K_m$. K_m value was increased but V_{max} remained unchanged with the increase of the daucosterol concentration, which was

consistent with the characteristics of the competitive inhibition model. The results suggested that α-glucosidase was inhibited by daucosterol in a competitive manner.

3.3 Fluorescence emission spectrum and synchronous fluorescence spectrum of α-glucosidase

The fluorescence quenching spectra of α-glucosidase by daucosterol are shown in Fig. 4A. The intrinsic fluorescence of tryptophan (Trp) and tyrosine (Tyr) residues was presented after excitation at the wavelength of 280 nm, α-glucosidase exhibited a strong fluorescence emission peak at 334.2 nm, the fluorescence intensity decreased with the increase of the concentration of daucosterol, and the maximum emission wavelength shifted from 334.2 nm to 336.0 nm, which showed a red-shift. The results indicated that daucosterol interacted with α-glucosidase and induced its intrinsic fluorescence quenching.

Table 2 Stern–Volmer quenching constants and binding parameters of the interaction between daucosterol and α-glucosidase at different temperatures

T (K)	K_q ($\times 10^{12}$ L mol^{-1} s^{-1})	K_A ($\times 10^4$ L mol^{-1})	ΔH° (kJ mol^{-1})	ΔS° (J mol^{-1} K^{-1})	ΔG° (kJ mol^{-1})
298	2.96	17.54	−52.89	−76.65	−29.92
303	2.51	14.27			−29.90
310	2.17	7.78			−29.03

The wavelength interval ($\Delta\lambda$) at 15 nm and 60 nm in the synchronous fluorescence spectra reflected the characteristic spectra of Tyr and Trp residues, respectively.[32] As seen in Fig. 4, the fluorescence intensity of the Tyr and Trp residues decreased significantly with the increase of the daucosterol concentration. The maximum emission wavelength of Tyr exhibited a red-shift (Fig. 4B), but the maximum emission wavelength of Trp was almost unchanged (Fig. 4C). These results suggested that daucosterol exhibited obvious intermolecular interactions with the active site of the Tyr residue of α-glucosidase.

3.4 The fluorescence quenching mechanism

The quenching process of enzyme fluorescence by an inhibitor can be divided into dynamic quenching and static quenching. The process follows the Stern–Volmer eqn (4), and the binding constant of the interaction between daucosterol and α-glucosidase was obtained using the modified Stern–Volmer eqn (5).[33]

$$\frac{F_0}{F} = 1 + K_q\tau_0[Q] = 1 + K_{sv}[Q] \tag{4}$$

$$\frac{F_0}{(F_0 - F)} = \frac{1}{f_A} + \frac{1}{f_A K_A[Q]} \tag{5}$$

where F_0 and F are the relative fluorescence intensity of the reaction system with and without quencher, respectively. K_q is the fluorescence quenching rate constant. τ_0 is the average lifetime of the fluorescent molecules without quencher, which is about 1×10^{-8} s. [Q] is the concentration of the quencher. K_{sv} is the dynamic quenching constant. K_A is the Stern–Volmer binding constant. f_A is the fractional maximum fluorescence intensity of the protein.

The Stern–Volmer linear-fitting graph of fluorescence quenching ($\lambda_{ex} = 280$ nm, $\lambda_{em} = 334$ nm) of α-glucosidase is shown in Fig. 4D. The quenching constants are summarized in Table 2. The values of K_A and K_q decreased with the increase of the temperature, and the K_q values were much higher than the maximum constant of the dynamic

Table 3 Binding energy of molecular docking between daucosterol and α-glucosidase[a]

Complex	Energy of molecular docking (kcal mol^{-1})						$\Delta G_{binding}$ (kcal mol^{-1})
	$E_{binding}$	E_{vdw}	E_{ele}	$E_{internal}$	$E_{torsional}$	E_{unbond}	
Daucosterol–α-glucosidase	−9.55	−13.00	−0.43	−3.39	3.88	−3.39	−9.55

[a] $E_{binding}$: predicted binding energy; E_{vdw}: van der Waals energy; E_{ele}: electrostatic energy; $E_{internal}$: total internal energy; $E_{torsional}$: torsional energy; E_{unbond}: unbound energy; $\Delta G_{binding}$: calculated binding energy. $\Delta G_{binding} = E_{vdw} + E_{ele} + E_{internal} + E_{torsional} - E_{unbond}$.
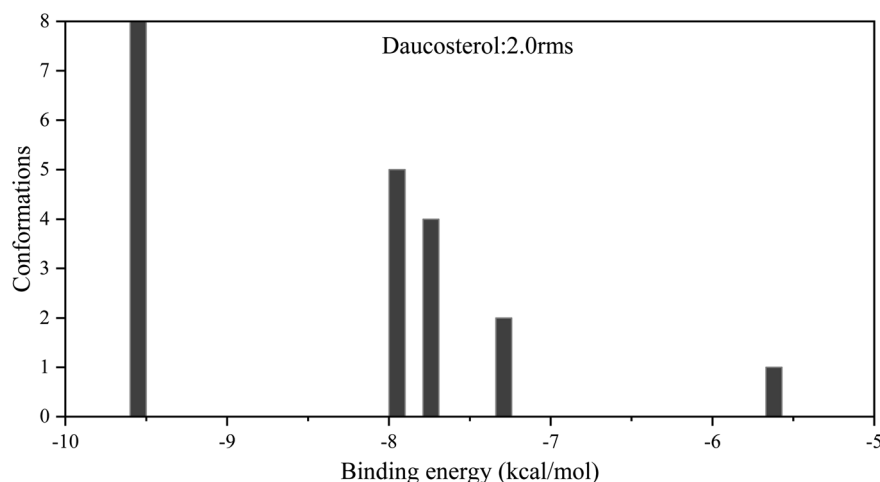
Fig. 5 Cluster analysis of conformations from the AutoDock docking runs of daucosterol with α-glucosidase.

fluorescence quenching of biomacromolecules (2×10^{10} L mol^{-1} s^{-1}), which was consistent with the characteristics of static fluorescence quenching.[34]

The thermodynamic constants of the interaction were obtained by the Van't Hoff equation (eqn (6)) and Gibbs free energy equation (eqn (7)) to reveal the binding process of daucosterol and α-glucosidase.

$$\ln K_{\mathrm{A}} = \frac{-\Delta H^{\circ}}{RT} + \frac{\Delta S^{\circ}}{R} \qquad (6)$$

$$\Delta G^{\circ} = \Delta H^{\circ} + T\Delta S^{\circ} \qquad (7)$$

In this equation, ΔH° is the enthalpy change of the reaction. ΔS° is the entropy change of the reaction. ΔG° is the Gibbs free energy change of the reaction. R is the molar gas constant (8.314 J mol^{-1} K^{-1}) and T is the thermodynamic temperature. As shown in Table 2, the value of ΔG° was negative, which demonstrated that the binding of daucosterol to α-glucosidase was a spontaneous process. ΔH° and ΔS° were negative,
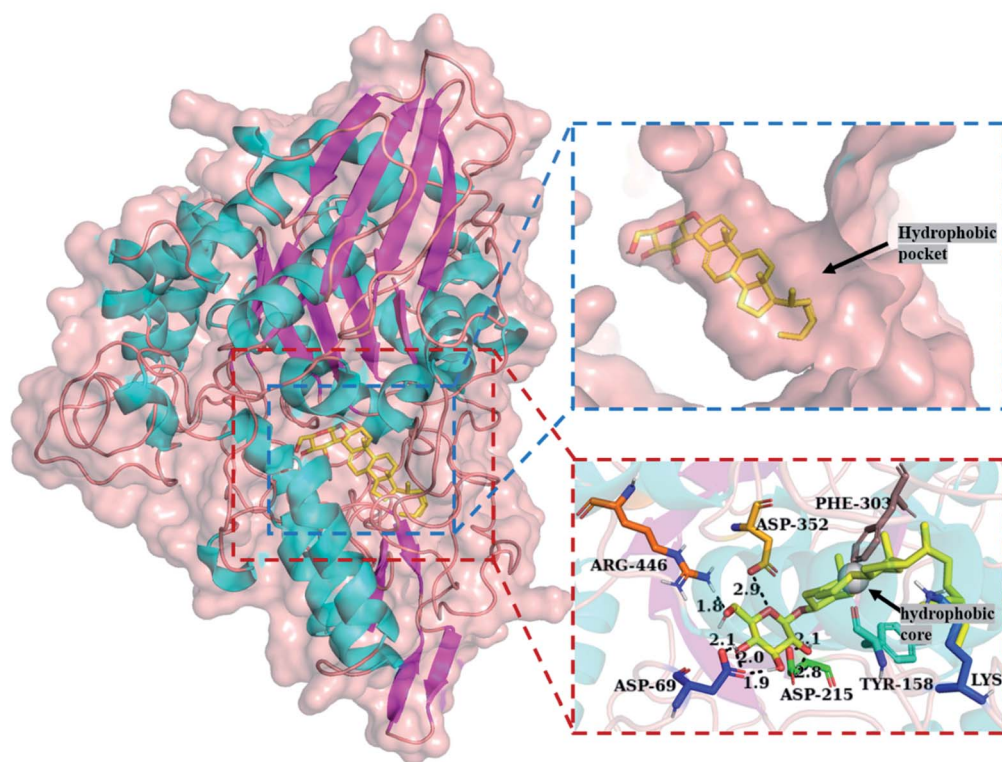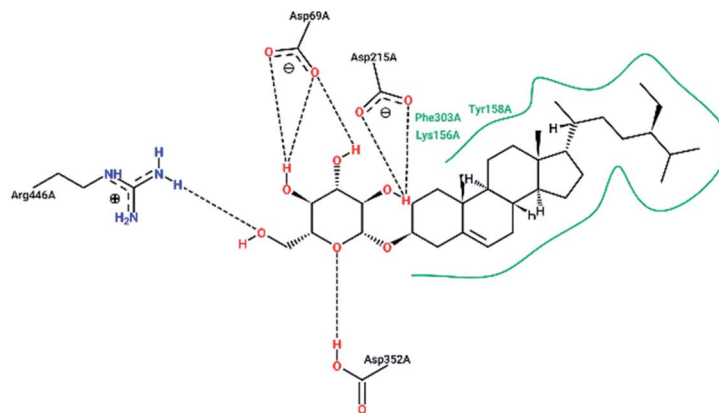

Fig. 6 Molecular docking analysis of α-glucosidase and daucosterol (A and B): 3D-diagram (A) and 2D-diagram (B) of molecular docking of daucosterol and α-glucosidase. The black dashed lines represent hydrogen-bonding interactions; the green solid line represents hydrophobic interactions.
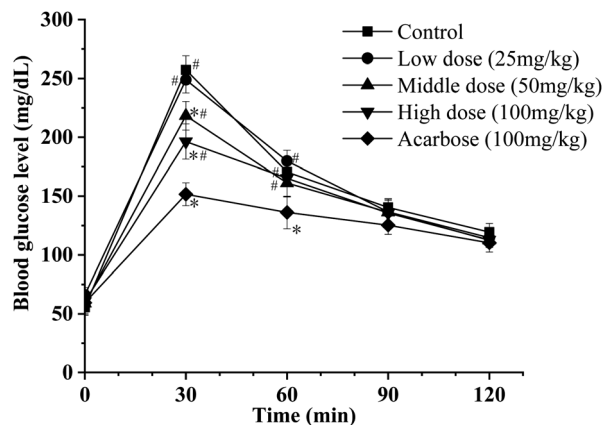
Fig. 7 The effect of daucosterol on the blood glucose level after maltose loading in mice. Values are means $\pm$ SEM, $n = 6$. $*p < 0.05$, compared with control group; $\#p < 0.05$, compared with acarbose group.

indicating that the binding energy was mainly derived from hydrogen bonds and van der Waals forces.[35]

3.5 Molecular docking analysis

The identity and the similarity of the amino acid sequences were obtained from the sequence alignment between α-glucosidase (GenBank: KZV11524.1) from *Saccharomyces cerevisiae* and isomaltase (PDB ID: 3AXI_A). The two proteins showed high identity (93%) and positivity (96%) in sequence (Fig. S3†), which indicated that 3AXI_A was able to provide a high-matched and high-quality 3D structure of α-glucosidase from *Saccharomyces cerevisiae* for homology modeling and molecular docking.

A cluster analysis of conformations from 20 docking runs was performed with the RMSD tolerance of 2.0 Å. The distribution map and results of binding energy from molecular docking between daucosterol and α-glucosidase are shown in Table 3 and Fig. 5. Five multimember conformational clusters were obtained in 20 conformations from molecule docking. The optimal cluster was the first with the lowest binding energy and contained 8 conformations. The intermolecular energy between daucosterol and α-glucosidase came primarily from van der Waals energy (-13.00 kcal mol^{-1}). The optimal binding energy was calculated as -9.55 kcal mol^{-1} and was consistent with the predicted binding energy, indicating that the docking result was credible.

The docking results are shown in Fig. 6, with daucosterol bound to the active site in the hydrophobic pocket of α-glucosidase. Hydroxyl groups on the glucopyranosyl residue of daucosterol formed seven hydrogen bonds with residues Asp 69, Asp 215, Asp 352 and Arg 446 of the binding site, including three for Asp 69, two for Asp 215, one for Asp 352 and one for Arg 446. Daucosterol aglycone also produced hydrophobic interactions with the residues of Lys 156, Tyr 158, and Phe 303 located at the exterior part of the binding pocket. Indeed, residues Asp 69, Asp 215 and Asp 352 were important catalytic residues in the active site of isomaltase.[36] However, daucosterol, as a monosaccharide derivative by sitosterol attachment to a β-

D-glucopyranosyl residue, was not able to be hydrolyzed by α-glucosidase. The results suggested that the inhibition mechanism of α-glucosidase by daucosterol was as follows: daucosterol bound to the hydrophobic pocket of α-glucosidase to block the entry of the substrate and changed the conformation of the active site to reduce the activity of α-glucosidase.

3.6 Inhibition of blood glucose increase

A maltose loading test was used to verify the inhibitory effect of daucosterol on α-glucosidase *in vivo*, and the blood glucose level of ddY mice is shown in Fig. 7. The blood glucose level of all mice increased significantly after administration of oral maltose, peaked at 30 min and then decreased. In the daucosterol-treated groups, the increased levels of blood glucose in the middle-dose group (50 mg kg^{-1}) and high-dose group (100 mg kg^{-1}) were lower than that in the control group at 30 min, and the results were statistically significant ($p < 0.05$). However, the blood glucose level of the acarbose group (100 mg kg^{-1}) increased slowly and was significantly lower than other groups at 30 and 60 min ($p < 0.05$). These results indicated that daucosterol inhibited the increase of blood glucose induced by maltose loading, but the inhibitory activity was weaker than that of acarbose.

4. Conclusion

Eleocharis dulcis is a common vegetable or fruit in Asia, and there are a variety of active constituents in its peel. In this research, three saponins were found in the methanol extract from *Eleocharis dulcis* peel for the first time, which were identified as stigmasterol glucoside, campesterol glucoside and daucosterol. The three saponins exhibited potent effective inhibitory activities against α-glucosidase compared with acarbose *in vitro*, and daucosterol possessed the strongest inhibition in a competitive manner. Fluorescence quenching of α-glucosidase was a static process caused by the formation of the daucosterol-α-glucosidase complex derived from hydrogen bonds and van der Waals forces. Molecular docking studies indicated that daucosterol formed seven hydrogen bonds with residues Asp 69, Asp 215, Asp 352 and Arg 446 in the active site of α-glucosidase, and produced hydrophobic interactions with residues Lys 156, Tyr 158 and Phe 303 located at the exterior part of the hydrophobic pocket.

As a α-glucosidase inhibitor, daucosterol inhibited the increase of blood glucose induced by maltose loading, which suggested that it could prevent the hydrolysis of maltose by α-glucosidase *in vivo*. However, the inhibition of α-glucosidase by daucosterol was weaker than that of acarbose. The difference of inhibition *in vitro* and *in vivo* might be due to the different reaction environment; for example, the strong acid, bile salts or intestinal flora in the digestive system might limit daucosterol from reaching its full potential *in vivo*. In general, the cost of medicine for the treatment of hyperglycemia is high, but *Eleocharis dulcis* peel with rich resources and low cost may be useful to develop potential hypoglycemic drugs.

Ethical statement

Ethical statements of living male ddY mice were obtained from Japan SLC, Inc. (Shizuoka, Japan). All animal procedures were performed in accordance with the 2006 guidelines entitled Notification No. 88 of the Ministry of the Environment in Japan and the Guidelines for Animals Experimentation of Tokyo University of Marine Science and Technology and approved by the Animal Care and Use Committee of Tokyo University of Marine Science and Technology. The investigation conformed to the Guide for the Care and Use of Laboratory Animals published by the US National Institutes of Health (NIH Publication No. 85-23, revised 1996).

Author contributions

This study was conducted and supported financially by associate professor Koyama. Materials, extraction and separation of crude saponins and detection of fluorescence quenching were supported by research associate Yang. Mr Shang and Ms Thao provided assistance with saponin purification and animal feeding operations.

Conflicts of interest

The authors state that there is no conflict of interest.

Acknowledgements

References

1 D. Odaci, A. Telefoncu and S. Timur, Maltose biosensing based on co-immobilization of α-glucosidase and pyranose oxidase, *Bioelectrochemistry*, 2010, **79**, 108–113.

2 E. D. Stefano, T. Oliviero and C. C. Udenigwe, Functional significance and structure-activity relationship of food-derived α-glucosidase inhibitors, *Curr. Opin. Food Sci.*, 2018, **20**, 7–12.

3 C. M. Santos, M. Freitas and E. Fernandes, A comprehensive review on xanthone derivatives as α-glucosidase inhibitors, *Eur. J. Med. Chem.*, 2018, **157**, 1460–1479.

4 M. Akaza, I. Akaza, T. Kanouchi, T. Sasano, Y. Sumi and T. Yokota, Nerve conduction study of the association between glycemic variability and diabetes neuropathy, *Diabetol. Metab. Syndr.*, 2018, **10**, 69.

5 Q. Wang, M. Rehman, D. Peng and L. Liu, Antioxidant capacity and α-glucosidase inhibitory activity of leaf extracts from ten ramie cultivars, *Ind. Crops Prod.*, 2018, **122**, 430–437.

6 H. Chen, K. Ouyang, Y. Jiang, Z. Yang, W. Hu, L. Xiong, N. Wang, X. Liu and W. Wang, Constituent analysis of the ethanol extracts of *Chimonanthus nitens Oliv.* leaves and their inhibitory effect on α-glucosidase activity, *Int. J. Biol. Macromol.*, 2017, **98**, 829–836.

7 J. Chen, L. Li, X. Zhou, B. Li, X. Zhang and R. Hui, Structural characterization and α-glucosidase inhibitory activity of polysaccharides extracted from Chinese traditional medicine Huidouba, *Int. J. Biol. Macromol.*, 2018, **117**, 815–819.

8 A. König, B. Schwarzinger, V. Stadlbauer, P. Lanzerstorfer, M. Iken, C. Schwarzinger, P. Kolb, S. Schwarzinger, K. Mörwald, S. Brunner, O. Höglinger, D. Weghuber and J. Weghuber, Guava (*Psidium guajava*) fruit extract prepared by supercritical CO_2 extraction inhibits intestinal glucose resorption in a double-blind, randomized clinical study, *Nutrients*, 2019, **11**, 1512.

9 L. Zhao, Y. Wang, G. Zhang, T. Zhang, J. Lou and J. Liu, L-Arabinose elicits gut-derived hydrogen production and ameliorates metabolic syndrome in C57BL/6J mice on high-fat-diet, *Nutrients*, 2019, **11**, 3054.

10 W. Benalla, S. Bellahcen and M. Bnouham, Antidiabetic medicinal plants as a source of alpha glucosidase inhibitors, *Curr. Diabetes Rev.*, 2010, **6**, 247–254.

11 V. Sekar, S. Chakraborty, S. Mani, V. K. Sali and H. R. Vasanthi, Mangiferin from *Mangifera indica* fruits reduces post-prandial glucose level by inhibiting α-glucosidase and α-amylase activity, *S. Afr. J. Bot.*, 2019, **120**, 129–134.

12 C. W. Choi, Y. H. Choi, M. R. Cha, D. S. Yoo, Y. S. Kim, G. H. Yon, S. K. Hong, Y. H. Kim and S. Y. Ryu, Yeast α-glucosidase inhibition by isoflavones from plants of Leguminosae as an in vitro alternative to acarbose, *J. Agric. Food Chem.*, 2010, **58**, 9988–9993.

13 D. Midmore, Chinese water chestnut, *The New Rural Industries Handbook: A Handbook for Farmers and Investors*, ed. K. Hyde, Rural Industries Research and Development Corporation, Canberra, Australia, 2004, pp. 181–187.

14 F. Islam, M. Faysal, T. A. Trina, M. Z. A. Begh, M. Al Amin, M. M. Rashid, M. M. Rahman, Phytochemical screening and anthelmintic activity of alcoholic extract of fruits of Eleocharis dulcis, PharmacologyOnLine, 2019, vol. 3, pp. 94–99.

15 Y. Luo, X. Li, J. He, J. Su, L. Peng, X. Wu, R. Du and Q. Zhao, Isolation, characterisation, and antioxidant activities of flavonoids from chufa (*Eleocharis tuberosa*) peels, *Food Chem.*, 2014, **164**, 30–35.

16 Y. You, X. Duan, X. Wei, X. Su, M. Zhao, J. Sun, N. Ruenroengklin and Y. Jiang, Identification of major phenolic compounds of Chinese water chestnut and their antioxidant activity, *Molecules*, 2007, **12**, 842–852.

17 X. Liu, L. Zhao and A. Zhou, Preliminary study on functional component and functional activities of waste slurry derived in processing water chestnut starch, *Food Sci.*, 2006, **27**, 251–256.

18 G. Zhan, L. Pan, K. Tu and S. Jiao, Antitumor, antioxidant, and nitrite scavenging effects of Chinese water chestnut (*Eleocharis dulcis*) peel flavonoids, *J. Food Sci.*, 2016, **81**, 2578–2586.

19 A. Baehaki, I. Widiastuti, S. Lestari, M. Masruro and H. A. Putra, Antidiabetic and anticancer activity of Chinese water chestnut (*Eleocharis dulcis*) extract with multistage extraction, *J. Adv. Pharm. Technol. Res.*, 2021, **12**, 40–44.

20 J. Vincken, L. Heng, A. De Groot and H. Gruppen, Saponins, classification and occurrence in the plant kingdom, *Phytochemistry*, 2007, **68**, 275–297.

21 V. S. Pires, A. T. Taketa, G. Gosmann and E. P. Schenkel, Saponins and sapogenins from *Brachiaria decumbens Stapf*, *J. Braz. Chem. Soc.*, 2002, **13**, 135–139.

22 J. L. C. Sright, A. G. McInnes, S. Shimizu, D. G. Smith, J. A. Walter, D. Idler and W. Khalil, Identification of C-24 alkyl epimers of marine sterols by ^{13}C nuclear magnetic resonance spectroscopy, *Can. J. Chem.*, 1978, **56**, 1898–1903.

23 P. L. Selmair and P. Koehler, Molecular structure and baking performance of individual glycolipid classes from lecithins, *J. Agric. Food Chem.*, 2009, **57**, 5597–5609.

24 S. Faizi, M. Ali, R. Saleem and S. Bibi, Complete ^{1}H and ^{13}C NMR assignments of stigma-5-en-3-O-β-glucoside and its acetyl derivative, *Magn. Reson. Chem.*, 2001, **39**, 399–405.

25 E. Kadowaki, Y. Yoshida, N. Baba and S. Nakajima, Feeding stimulative activity of steroidal and secoiridoid glucosides and their hydrolysed derivatives toward the olive weevil (*Dyscerus perforatus*), *Z. Naturforsch., C: J. Biosci.*, 2003, **58**, 441–445.

26 L. Zhang, S. Hogan, J. Li, S. Sun, C. Canning, S. J. Zheng and K. Zhou, Grape skin extract inhibits mammalian intestinal α-glucosidase activity and suppresses postprandial glycemic response in streptozocin-treated mice, *Food Chem.*, 2011, **126**, 466–471.

27 Y. Si, Z. Wang, D. Park, H. Y. Chung, S. Wang, L. Yan, J. Yang, G. Qian, S. Yin and Y. Park, Effect of hesperetin on tyrosinase: inhibition kinetics integrated computational simulation study, *Int. J. Biol. Macromol.*, 2012, **50**, 257–262.

28 P. Nussbaumer, A. Winiski, S. Cammisuli, P. Hiestand, G. Weckbecker and A. Stutz, Novel antiproliferative agents derived from lavendustin A, *J. Med. Chem.*, 1994, **37**, 4079–4084.

29 E. Laine, C. Goncalves, J. C. Karst, A. Lesnard, S. Rault, W. J. Tang, T. E. Malliavin, D. Ladant and A. Blondel, Use of allostery to identify inhibitors of calmodulin-induced activation of Bacillus anthracis edema factor, *Proc. Natl. Acad. Sci. U. S. A.*, 2010, **107**, 11277–11282.

30 N. Ghosh, R. Mondal and S. Mukherjee, Hydrophobicity is the governing factor in the interaction of human serum albumin with bile salts, *Langmuir*, 2015, **31**, 1095–1104.

31 P. A. Zunszain, J. Ghuman, T. Komatsu, E. Tsuchida and S. Curry, Crystal structural analysis of human serum albumin complexed with hemin and fatty acid, *BMC Struct. Biol.*, 2003, **3**, 1–9.

32 S. Rubio, A. Gomezhens and M. Valcarcel, Analytical applications of synchronous fluorescence spectroscopy, *Talanta*, 1986, **33**, 633–640.

33 J. R. Lakowicz, *Principles of fluorescence spectroscopy*, Springer Sci Bus Media, 2013, pp. 278–289.

34 J. Yan, G. Zhang, J. Pan and Y. Wang, α-Glucosidase inhibition by luteolin: kinetics, interaction and molecular docking, *Int. J. Biol. Macromol.*, 2014, **64**, 213–223.

35 P. D. Ross and S. Subramanian, Thermodynamics of protein association reactions: forces contributing to stability, *Biochemistry*, 1981, **20**, 3096–3102.

36 K. Yamamoto, H. Miyake, M. Kusunoki and S. Osaki, Steric hindrance by 2 amino acid residues determines the substrate specificity of isomaltase from *Saccharomyces cerevisiae*, *J. Biosci. Bioeng.*, 2011, **112**, 545–550.